

The Study of Physics from Phase Transitions to Living Matter

The Study of Physics from Phase Transitions to Living Matter

By

Isabel M. Irurzun and Leopoldo Garavaglia

**Cambridge
Scholars
Publishing**



The Study of Physics from Phase Transitions to Living Matter

By Isabel M. Irurzun and Leopoldo Garavaglia

This book first published 2023

Cambridge Scholars Publishing

Lady Stephenson Library, Newcastle upon Tyne, NE6 2PA, UK

British Library Cataloguing in Publication Data

A catalogue record for this book is available from the British Library

Copyright © 2023 by Isabel M. Irurzun and Leopoldo Garavaglia

All rights for this book reserved. No part of this book may be reproduced, stored in a retrieval system, or transmitted, in any form or by any means, electronic, mechanical, photocopying, recording or otherwise, without the prior permission of the copyright owner.

ISBN (10): 1-5275-0438-7

ISBN (13): 978-1-5275-0438-7

CONTENTS

Preface	vii
Chapter 1	1
Changes of state in pure substances	
Chapter 2	11
Phase transitions in crystalline solids	
Chapter 3	23
Phase transitions on crystalline surfaces	
Chapter 4	30
Phase transitions in alloys	
Chapter 5	39
Phase transitions in magnetic systems	
Chapter 6	55
Phase transitions in liquid crystals	
Chapter 7	67
Phase transitions in polymers	
Chapter 8	78
Phase transitions in quantum systems	
Chapter 9	92
Critical behaviour and phase transitions	
Chapter 10	106
Critical behaviour in out-of-equilibrium systems	
Chapter 11	121
Critical behaviour and fractality	

Chapter 12	134
Dynamical systems	
Chapter 13	149
Complex systems and living matter	
Bibliography	156

PREFACE

This book was thought for a wide population of undergraduate and graduate students in science, and more specifically in physics. The text is written in a very didactic way, covering a wide range of topics in the field of phase equilibrium. It is in a comprehensible language, without loss of the proper rigour from the scientific point of view.

The text describes different aspects of phase equilibrium, from simple to more complex systems, such as liquid crystals, polymers, superconductivity and superfluidity, growth of interfaces, fractals, non-linear systems, chaos and self-organization. One of the aims of the authors is to present the basic characteristics of the living systems, without considering the origin of life itself. The description of the different topics is supported as far as possible by experimental and theoretical concepts arising from physics, mathematics, and physical and biophysical chemistry, which can be applied in biology, biochemistry and environmental sciences.

The authors cover these topics from Chapter 1 to Chapter 13. They start from the phase equilibrium of simple substances and the thermodynamic requirement based on the chemical potential for deducing the basic equations (such as Clapeyron and Clausius Clapeyron equations), and then describe several types of equilibrium, until Chapter 7, where the statistical aspects of macromolecular systems are considered. More advanced topics are developed from Chapter 8 to 12. The phase transitions in quantum systems are presented in a didactic approach in comparison with other treatments described in the literature.

Finally, the ideas developed in the previous chapters, such a self-organization, chaos and fractality are exposed to analyse those processes in biological systems. In Chapter 13 the authors present their own ideas about the factors that are relevant in interpreting the basic aspects of the living systems.

The diagrams, figures and examples are well presented and they contribute to a better understanding of the different topics developed in the text. The references are wide, classic and modern.

The authors demonstrate their experience in teaching and research in the different fields presented in the book. Several of the experiments, calculations or models are the result of their research in these areas and open up several questions for further research in the field.

—A.L. Capparelli

CHAPTER 1

CHANGES OF STATE IN PURE SUBSTANCES

1.1 Introduction

Pure substances can be found in nature in various aggregation states depending on temperature (T), pressure (P) or any external intensive variable that influences them. The most common aggregation states are: solid (with various allotropic forms), liquid, and gaseous. A sample of a pure substance will evolve spontaneously, decreasing its chemical potential (μ). However, we must remember that this alternative way of expressing the spontaneous evolution of a system originates in the tendency of the universe to an ever increasing disorder.

The most stable aggregation state will have the lowest chemical potential (at given values of temperature and pressure), and a sample of a substance will evolve towards that state. For example, the sample will tend to evaporate if the chemical potential of the gas is less than that of the liquid. If the chemical potentials of two aggregation states are equal, both states coexist in equilibrium, and we say that the system has two phases.

A phase is a portion of the system having uniform intensive properties, for example, a liquid phase always has the same density, regardless of the portion of liquid that we consider. This liquid phase is distinguished from the gas phase because it has a different density and, in general, other intensive properties are also different.

Fig. 1.1 shows the typical dependence of the chemical potential on temperature of the solid, liquid, and gas states of a pure substance. The slopes of the curves determine the molar entropy (s) according to the equation

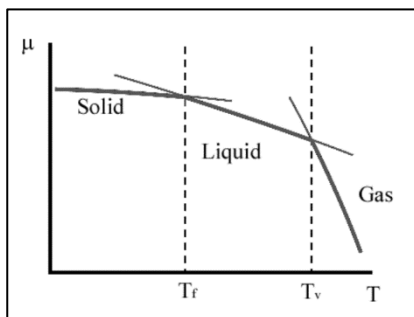


Figure 1.1: Dependence of the chemical potential on temperature of the solid, liquid, and gas states of a pure substance (Atkins and de Paula 2006).

$$\left(\frac{\partial\mu}{\partial T}\right)_P = -s$$

The chemical potential also depends on pressure and

$$\left(\frac{\partial\mu}{\partial P}\right)_T = v$$

where v is the molar volume, also an intensive property of a pure substance, which takes different values in the various aggregation states.

Phase diagrams are representations showing the regions of pressure and temperature (and any other intensive properties that affect the state of a substance) where the solid, liquid, and gas phases are stable. These phases are generally represented by their molar volume. The phase diagrams of pure substances have at least three dimensions (V , P , and T).

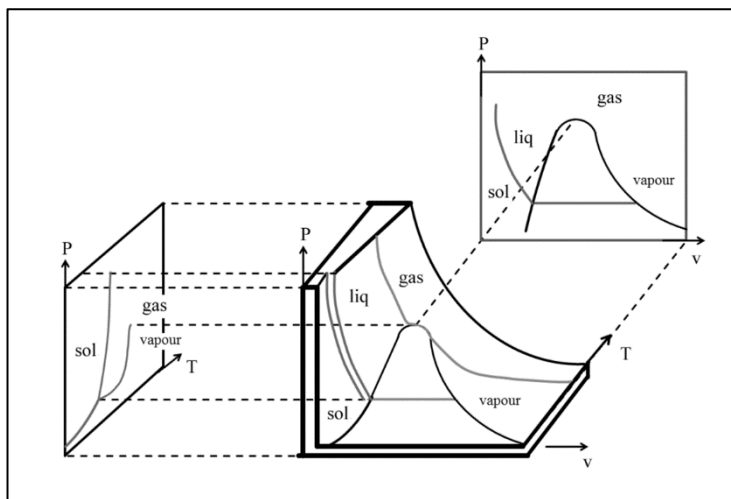


Figure 1.2: Typical three-dimensional phase diagram and its two more often used two-dimensional projections.

Fig. 1.2 shows a typical phase diagram. For simplicity, two-dimensional projections are often used in the P - T and P - V planes (Fig. 1.3).

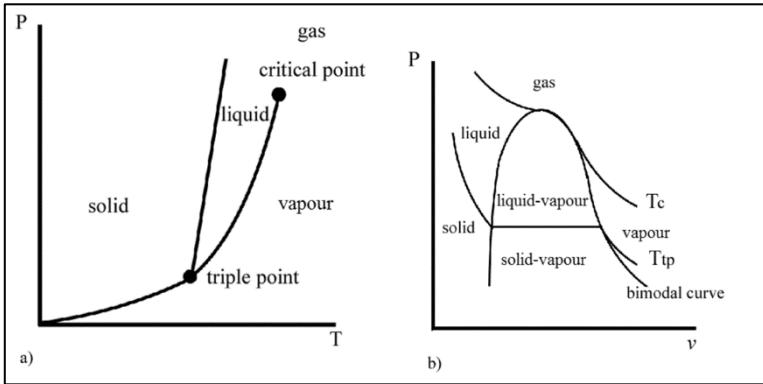


Figure 1.3: $P-T$ (a) and $P-v$ (b) diagrams, with typical two-phase and three-phase coexistence regions.

In the $P-T$ diagram, the triple point and the critical point can be distinguished. At the triple point, the three aggregation states coexist in equilibrium. The critical point marks the end of the coexistence curve between the liquid and the vapour. Above the critical temperature (T_c), the densities (or the molar volumes) of the liquid and of the vapour are equal ($\delta_l = \delta_g$, $v_l = v_g$). Solid lines in Fig. 1.3a indicate the coexistence conditions of two phases.

The Clapeyron equation allows obtaining an expression for these limits

$$\frac{dP}{dT} = \frac{\Delta s}{\Delta v}$$

By considering the relationship between entropy and enthalpy (H) at melting, sublimation, and vaporization temperatures (at constant pressure), specific expressions are derived for each of the lines.

Solid-liquid boundary

$$\frac{dP}{dT} = \frac{\Delta H_{mm}}{T\Delta v_m}$$

This equation can be integrated by neglecting the dependence of Δv_m on temperature and taking the triple point (tp) as a reference

$$P = P_{tp} + \left(\frac{\Delta H_{mm}}{\Delta v_m} \right) \ln \left(\frac{T}{T_{tp}} \right)$$

Liquid-gas boundary

$$\frac{dP}{dT} = \frac{\Delta H_{mv}}{T\Delta v_v}$$

Since the molar volume of a gas is greater than that of a liquid, we can write $\Delta v_v = v_g$ and also suppose that steam behaves like an ideal gas, so that $v_g = \frac{RT}{P}$. These approximations lead to the Clausius-Clapeyron equation

$$\frac{d(\ln P)}{dT} = \frac{\Delta H_{mv}}{RT^2}$$

that can be integrated taking the triple point as a reference

$$P = P_{tp} \exp \left[-\frac{\Delta H_{mv}}{R} \left(\frac{1}{T} - \frac{1}{T_{tp}} \right) \right]$$

Solid-gas boundary

The above approaches can be made at this border. Clausius-Clapeyron equation is now

$$P = P_{tp} \exp \left[-\frac{\Delta H_{ms}}{R} \left(\frac{1}{T} - \frac{1}{T_{tp}} \right) \right]$$

Fig 1.3b shows the P - V phase diagrams. Below the critical temperature (T_c), the liquid-gas coexistence region reveals discontinuities in the molar volume. The same occurs in the solid-vapour coexistence zone. At high temperatures and low pressures, the isotherms resemble those predicted by the ideal gas law

$$Pv = RT$$

At low temperatures and high pressures, all real gases exhibit deviations from ideal behaviour. The molecular origin of the deviations is the interaction between particles, and one way to quantify them is through the virial equations of state

$$Pv = RT \left\{ 1 + B/v + C/v^2 + \dots \right\}$$

where B , C , etc. are known as the second, third, etc. virial coefficients.

Deviations from ideal behaviour can also be expressed in terms of the compressibility factor

$$Z = \frac{Pv}{RT}$$

for an ideal gas $Z = 1$, and its deviation is a measure of the imperfection of the gas. Fig. 1.4a shows the Z values for various gases at various temperatures. These apparently so different curves can be joined if the reduced variables are considered as in Fig 1.4b

$$T_r = \frac{T}{T_c}$$

$$P_r = \frac{P}{P_c}$$

$$v_r = \frac{v}{v_c}$$

This behaviour agrees with Van der Waals' idea that gases confined in the same reduced volume and at the same reduced temperature would exert the same reduced pressure. This observation is also known as the law of corresponding states and is an example of what we will call universal behaviour.

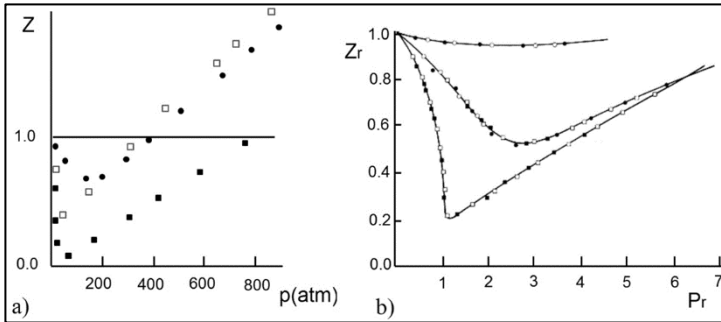


Figure 1.4: (a) Z values for different real gases: nitrogen (circles), propane (open squares), ethene (filled squares). (b) The law of corresponding states: the curves in a) collapse into master curves by using reduced variables. Each curve in (b) corresponds to a given reduced temperature (Atkins and de Paula 2006).

1.2 Four real systems

The experimental phase diagram of water is shown in Fig. 1.5. The solid-liquid curve summarizes the dependence of the melting temperature on pressure. At low pressures the slope is negative because $\Delta v_f < 0$, i.e. the water contracts when melting, or the density of the solid (ice) is lower than that of the liquid, and therefore ice floats. Indeed, the crystal lattice of ice is very open, stabilized by hydrogen bonds. At higher pressures other crystalline structures are stable, giving rise to different types of ice.

Fig. 1.6 shows the phase diagram of carbon dioxide (CO_2). The coexistence lines show the characteristic behaviour. The triple point is found at values higher than the normal pressure of 1atm, thus in this condition, CO_2 sublimates going from solid to gas.

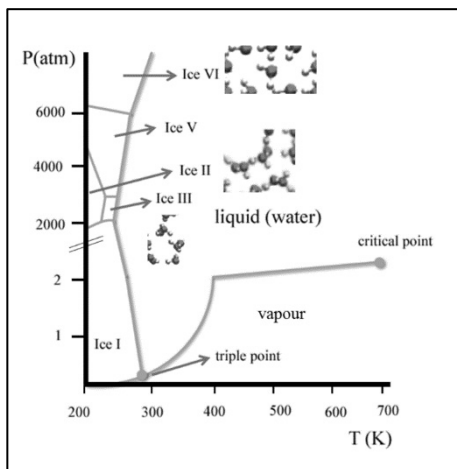


Figure 1.5: P-T phase diagram of pure water. Note the different types of ice (Atkins and de Paula 2006).

The phase diagram of carbon is shown in Fig 1.7. Under normal pressure and temperature conditions, the thermodynamically stable phase is graphite. This means that a diamond piece should spontaneously transform into graphite. For this to happen, the crystalline structure must change. Although this change is spontaneous, it is extremely slow to be perceptible on the time scales of human life.

Fig. 1.8 shows the ^4He phase diagram. Helium behaves in an unusual way at low temperatures. For example, the solid and gas phases never coexist. Instead, there are two liquid phases that coexist with the gas at the triple point. The liquid (I) phase has the usual characteristics of a liquid, while the liquid (II) phase is superfluid, it flows with zero viscosity. The phenomenon of superfluidity will be discussed in Chapter 8.

1.3 Thermodynamics of phase transitions

Phase transitions occur with abrupt changes in the intensive properties of the system. Fig. 1.1 shows the changes in chemical potential (the molar Gibbs energy) with temperature. This function is mathematically continuous, but its derivative has a discontinuity that indicates the phase transition.

The following equations relate the chemical potential and its derivatives to the other thermodynamic quantities in processes involving a pure substance

$$d\mu = v dP - s dT$$

$$\left(\frac{\partial\mu}{\partial T}\right)_P = -s$$

$$\left(\frac{\partial\mu}{\partial P}\right)_T = v$$

$$(dH_m)_P = T ds$$

$$C_{m,p} = \left(\frac{\partial H_m}{\partial T}\right)_P = T \left(\frac{\partial^2\mu}{\partial T^2}\right)_P$$

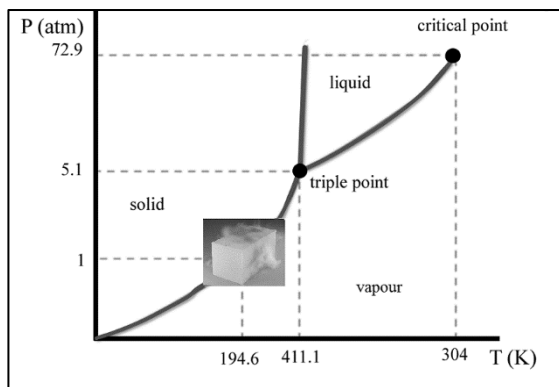


Figure 1.6: Phase diagram of carbon dioxide (CO₂) (Atkins and de Paula 2006).

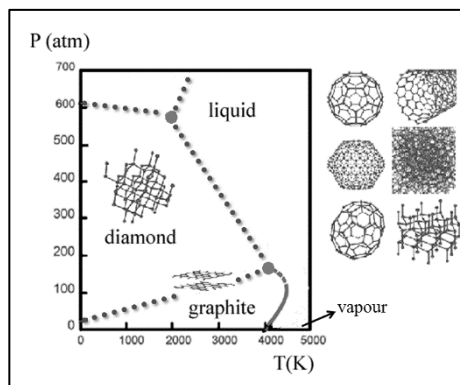


Figure 1.7: Phase diagram of carbon and different phases including those obtained in laboratory conditions (fullerenes, nanotube, amorphous phase, and lonsdaleite) (Atkins and de Paula 2006).

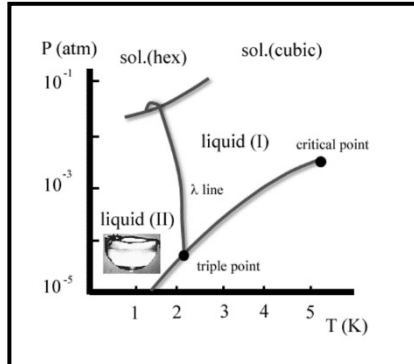


Figure 1.8: Phase diagram of pure helium. Liquid (I) is a normal liquid, while liquid (II) is a superfluid (Atkins and de Paula 2006).

Fig. 1.9a shows how these magnitudes vary in phase transitions such as solidification, sublimation, condensation, etc. The first derivatives of the chemical potential are discontinuous, and for this reason they are called first-order phase transitions. In these transitions the heat capacity tends to infinity at the transition temperature.

Continuous phase transitions are changes in which discontinuities occur in the second derivatives of the chemical potential.

In the second-order phase transitions (Fig. 1.9b) the heat capacity takes on finite values at both sides of the critical point. Second-order transitions are: the order-disorder transitions in alloys, the conductor-superconductor transition in the absence of a magnetic field.

In lambda transitions the heat capacity tends to infinity only from lower than critical values. A characteristic lambda transition is the fluid-superfluid transition in ^4He .

This classification of phase transitions is a reasonable generalization of the Ehrenfest criteria.

Currently, the classification of phase transitions is more elaborate and we will present it throughout this text. This starting point, however, allows us to establish some basic concepts that we will gradually generalize and discuss below.

First-order phase transitions can be detected by analysing the dependence of the molar volume or density of the system on temperature. We then have a control parameter (temperature) which is an intensive quantity that can be externally varied to modify the state of the system. Eventually, the control parameter may be pressure, magnetic field, etc. We

will say that the control parameter takes its critical value if it takes the value at which the phase transition occurs. This term generalizes the critical point concept used previously.

The free energy of the system, and then its Hamiltonian, must depend on the order parameter. The importance of this statement will be revealed later.

In phase transitions, the order parameter undergoes an abrupt change at the critical point. We say that the system changes from an ordered state (associated with an order parameter value greater than zero) to a disordered state (associated with an order parameter value equal to zero).

For the transitions studied in this chapter, the order parameter is

$$\varphi = \delta_l - \delta_g$$

Critical opalescence is an optical phenomenon that can be observed at the liquid-gas interface near the critical point. It is associated with fluctuations in density (or the order parameter). Both behaviours will be discussed later.

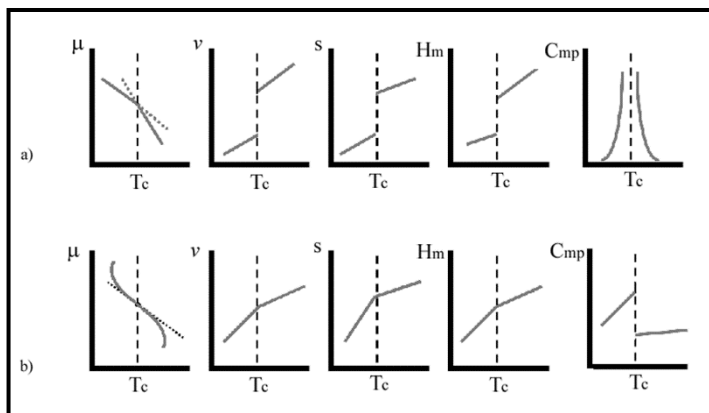


Figure 1.9: Variation of the thermodynamic variables with temperature near the critical point. (a) First-order phase transition, (b) second-order phase transition (Atkins and de Paula 2006).

CHAPTER 2

PHASE TRANSITIONS IN CRYSTALLINE SOLIDS

2.1 Perfect crystalline solids

Many phase transitions in crystalline solids are of first order such as those studied in Chapter 1. The crystalline structure changes in the transition; the control parameters are temperature and pressure (T, P). In this chapter we discuss some basic concepts of crystallography and solid state theory (Ashcroft and Mermin, 1976). The discussion will be focused on the concept of order, while its variations will be addressed in the next chapters. We also present one of the most important experimental techniques of the 20th century in this discipline, X-ray diffraction.

A perfect crystalline solid has infinite translational symmetry. Let us consider a regular arrangement of points in space, as shown in Fig. 2.1, and let \vec{a} , \vec{b} , and \vec{c} be three vectors that define a unit cell. The translational symmetry condition is expressed as

$$\vec{R}_m = \vec{R}_0 + \vec{t}_m$$
$$\vec{t}_m = m_1\vec{a} + m_2\vec{b} + m_3\vec{c}$$

where m_1, m_2, m_3 are integer numbers.

A unit cell is one that is capable of generating the crystal lattice by translation. If the unit cell also contains a single point of the lattice, it is called a primitive cell.

The Voronoi or Wigner-Seitz cell is a primitive cell constructed from the bisectors to the segments, joining an atom with its neighbours (Fig. 2.2).

A perfect crystalline solid can be described with a single Wigner-Seitz cell. If instead an infinite number of different cells are required, the solid is amorphous, (there is no crystalline arrangement). A finite number of Wigner-Seitz cells are found in polycrystals and quasicrystals.

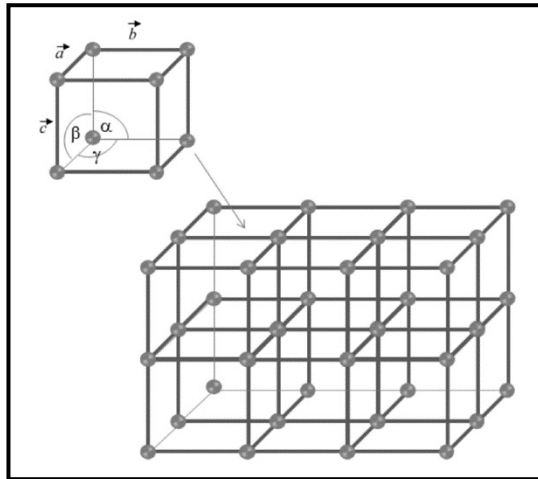


Figure 2.1: A Wigner-Seitz primitive cell constructed for an arbitrary arrangement of points

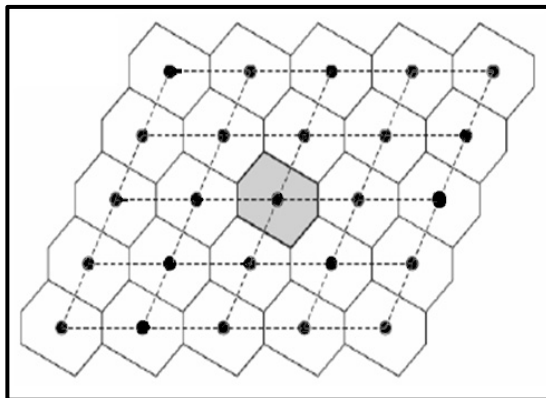


Figure 2.2: A perfect crystalline solid is generated by the translation of a single unit cell defined by three vectors.

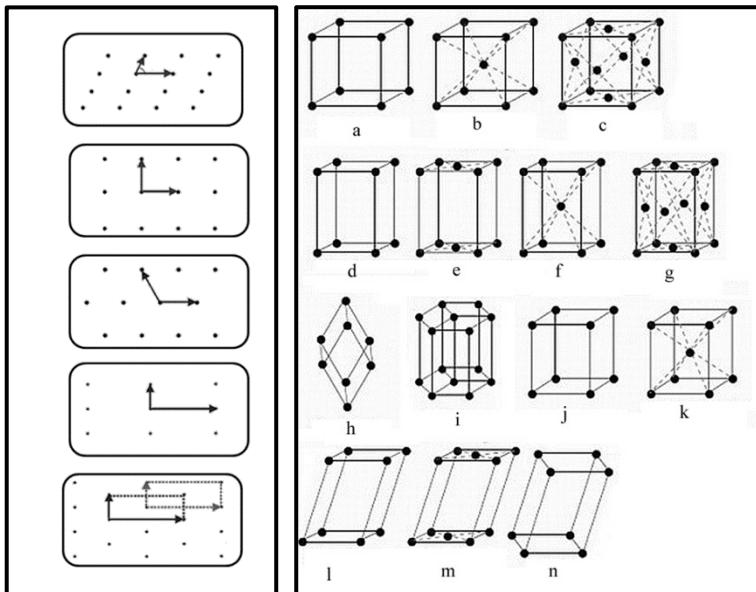


Figure 2.3 (left): The five Bravais lattices in a two-dimensional geometry. From top to bottom: oblique, square, hexagonal, rectangular, centred rectangular.

Figure 2.4 (right): The 14 Bravais lattices in three dimensions: (a) simple cubic, (b) body-centred cubic, (c) face-centred cubic, (d) simple orthorhombic, (e) base-centred orthorhombic, (f) body-centred orthorhombic, (g) face-centred orthorhombic, (h) rhombohedral, (i) hexagonal, (j) tetragonal, (k) body-centred tetragonal, (l) simple monoclinic, (m) base-centred monoclinic, (n) triclinic.

In geometry and crystallography, the Bravais lattices are arrangements of discrete points whose structure is invariant under a certain group of translations. In most cases they also present rotational symmetry. These properties make that the perspective of the lattice be the same from each node of a Bravais lattice, i.e. the points of a Bravais lattice are all equivalent.

Group theory has shown that there is only a single one-dimensional Bravais lattice, 5 two-dimensional lattices (Fig. 2.3), and 14 different three-dimensional Bravais lattices (Fig. 2.4).

Bravais lattices are grouped into crystal systems according to symmetry operations. Fig. 2.5 shows the crystal systems with their Bravais lattices in 3D.

More complex crystal structures can be described in terms of a periodic arrangement of a basis element.

An important concept in crystallography refers to Miller's indices, which are used to indicate crystallographic plane orientations. Miller's indices are indicated by the letters (h, k, l).

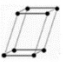
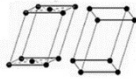
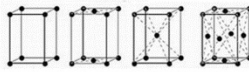
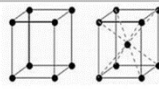
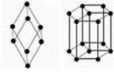
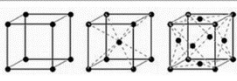
Crystal system	Bravais Lattices
Triclinic	
Monoclinic	
Orthorhombic	
Tetragonal	
Hexagonal	
Cubic	

Figure 2.5: Crystal systems and their corresponding Bravais lattices in 3D.

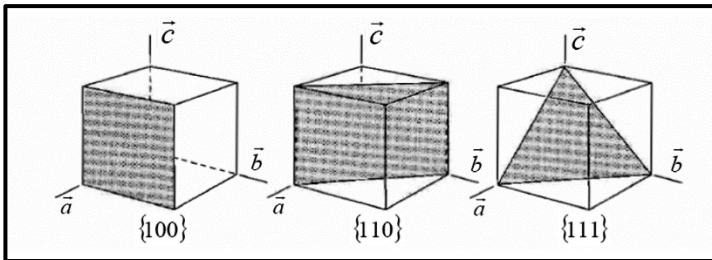


Figure 2.6: The crystallographic plane orientations are indicated by the Miller's indices, which are given between brackets below each example in the figure.

To obtain them we first determine the intersection points of the plane with the coordinate system axes (Fig. 2.6).

Let (m, n, p) be these intersection points, the indices (h, k, l) are

$$h = \frac{A}{m}, k = \frac{A}{n}, l = \frac{A}{p}$$

where A is the least common multiple of (m, n, p) .

Index zero corresponds to a plane parallel to an axis. Negative index will be indicated with a hyphen above it. If the plane passes through the origin, it will move to an equivalent position in the cell. A family of planes will be indicated by enclosing the indices in braces $\{h, k, l\}$.

2.2 X-ray diffraction

Diffraction is an optical phenomenon that allows the identification and study of the characteristics of a regular array of points. It can be experimentally observed when a small obstacle or slit is illuminated with coherent radiation of wavelength (λ) similar to the object size. Two slits spaced a small distance (d) apart produce the interference pattern shown in Fig. 2.7.

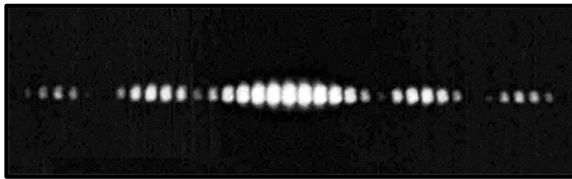


Figure 2.7: A typical interference pattern of two slits. The intensity of each spot of light is modulated by the diffraction pattern of a single slit.

A set of many point slits constitute a diffraction lattice, which produces intense lines of light. The line positions depend on the wavelength of the incident light and the distance between the slits, and are given by

$$d \sin \theta_n = \pm n \lambda$$

where n is an integer.

In a crystal lattice, the cell size is about 1\AA (10^{-10}m), so the corresponding wavelength is in the X-ray region of the electromagnetic spectrum. The energy involved is calculated as

$$E = h \frac{c}{\lambda} = 12\text{KeV}$$

where c is the speed of light in vacuum and h the Planck constant.

Subatomic particles are also used in diffraction experiments as they exhibit dual behaviour.

Neutron diffraction is used to study crystal structures with magnetic properties or light elements. These particles do not interact with the electrons of the crystalline solid but directly with the nuclei. Neutron beams are generated in nuclear reactors, and the required energy is calculated as

$$E = \frac{p^2}{2m} = \frac{1}{2m} \left(\frac{h}{\lambda} \right)^2$$

where p is the neutron momentum and m is its mass.

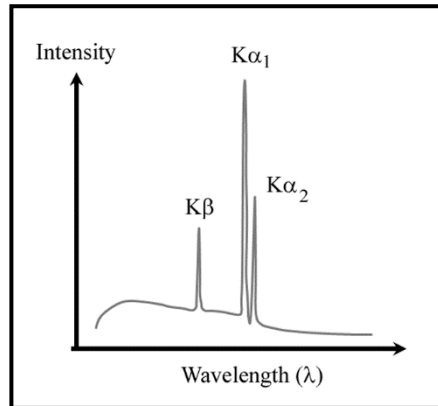


Figure 2.8: A typical X-ray spectrum produced in an X-ray tube. The background is a continuous spectrum called Bremsstrahlung spectrum. Monochromatic beams are $K_{\alpha 1}$, $K_{\alpha 2}$, and K_{β} , whose wavelengths depend on the chemical nature of the target in the tube (Pecharsky and Zavalij, 2009).

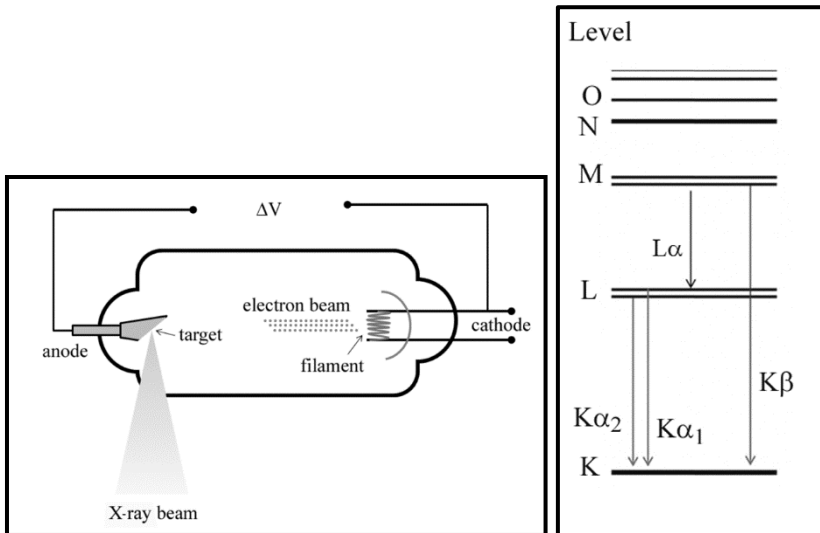


Figure 2.9 (left): Scheme of an X-ray tube

Figure 2.10 (right): Monochromatic X-rays are generated by de-excitation of inner layer electrons of the target in an X-ray tube. The nomenclature considers the energy levels involved.

Electron diffraction is used to study surface structures. These particles strongly interact with the electrons of the crystalline solid and penetrate just a few atomic layers.

X-rays are generated due to deceleration of a very energetic electron beam ($E \sim 10 \text{ KeV}$) that collides with a metallic target. This deceleration produces a continuous X-ray spectrum, the "braking radiation" or Bremsstrahlung. In addition, the atoms of the metallic material also emit monochromatic X-rays. These characteristic emission lines of the material are used in diffraction experiments (Fig. 2.8).

X-rays are produced in laboratories by using X-ray tubes. They are made up of two electrodes (cathode and anode); a filament to release electrons and a target inside a glass evacuated envelope (Fig. 2.9).

The electrons are accelerated through a potential difference (ΔV) between the cathode and the anode. Radiation occurs in the electron impact zone and is emitted in all directions.

The energy of the electrons is

$$E = e\Delta V$$

where e is the magnitude of the electron charge.

Monochromatic X-rays are generated when incident electrons excite inner layer electrons of target atoms. Subsequent de-excitation produces specific wavelength radiation dependent on the chemical composition of the target. X-ray emissions are designated as K, L, etc., as shown in Fig. 2.10.

The diffraction condition in crystallography is known as Bragg's Law

$$2d\sin\theta_n = \pm n\lambda$$

In Laue's formulation, each point of a crystal lattice can be considered as a scattering centre of radiation. The scattering does not change the frequency of the radiation.

We represent a radiation wave as $e^{i\vec{k}\cdot\vec{r}}$, with $\vec{k} = \frac{2\pi}{\lambda}\vec{k}$. According to Fig. 2.11, the total constructive interference condition for two points is

$$d\sin\theta + d\sin\theta' = \vec{d}\cdot(\vec{k} - \vec{k}') = n\lambda$$

$$\vec{d}\cdot(\vec{k} - \vec{k}') = 2\pi n$$

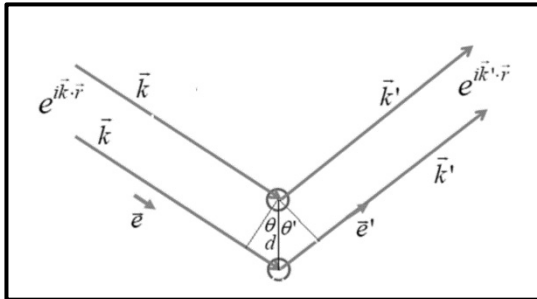


Figure 2.11: Scattering of radiation in a crystal lattice. The optical path difference causes a phase difference so that only waves scattered at specific angles interfere constructively (Laue's condition) (Pecharsky and Zavaliij, 2009).

where n is integer. The condition for the whole crystal lattice is

$$\vec{t}_m \cdot (\vec{k} - \vec{k}') = 2\pi n$$

$$e^{i\vec{t}_m \cdot (\vec{k} - \vec{k}')} = 1$$

This is the condition for constructive interference or Laue's condition.

2.3 Description in the reciprocal space

The reciprocal lattice plays a fundamental role in most analytic studies of periodic structures, particularly in the theory of diffraction.

We can define a vector $\vec{K} = \vec{k} - \vec{k}'$ so that

$$\vec{K}_{m'} = m'_1 \vec{a}^* + m'_2 \vec{b}^* + m'_3 \vec{c}^*$$

where m'_1, m'_2 and m'_3 are integers and

$$\vec{a}^* = 2\pi \frac{\vec{b} \times \vec{c}}{\vec{a} \cdot (\vec{b} \times \vec{c})}, \vec{b}^* = 2\pi \frac{\vec{c} \times \vec{a}}{\vec{a} \cdot (\vec{b} \times \vec{c})}, \vec{c}^* = 2\pi \frac{\vec{a} \times \vec{b}}{\vec{a} \cdot (\vec{b} \times \vec{c})}$$

Then Laue's condition is fulfilled since

$$\vec{K}_{m'} \cdot \vec{t}_m = 2\pi(m'_1 m_1 + m'_2 m_2 + m'_3 m_3)$$

We say that a^* , b^* , and c^* are the primitive vectors that generate the reciprocal space to which $\vec{K}_{m'}$ vectors belong.

Any crystal can be described by a lattice in the direct space or by one in the reciprocal space. Both descriptions are equivalent and contain exactly the same information.

We observe the direct lattice with microscopy techniques, which allow us to identify each of the atoms that make up the lattice. The reciprocal lattice is observed in the diffraction image of the crystal.

As $\vec{K}_{m'} = \vec{k} - \vec{k}'$ and $|\vec{k}| = |\vec{k}'|$, then $\vec{k} \cdot \vec{K}_{m'} = \frac{1}{2} |\vec{K}_{m'}|^2$. This condition defines the Bragg planes, as shown in Fig. 2.12.

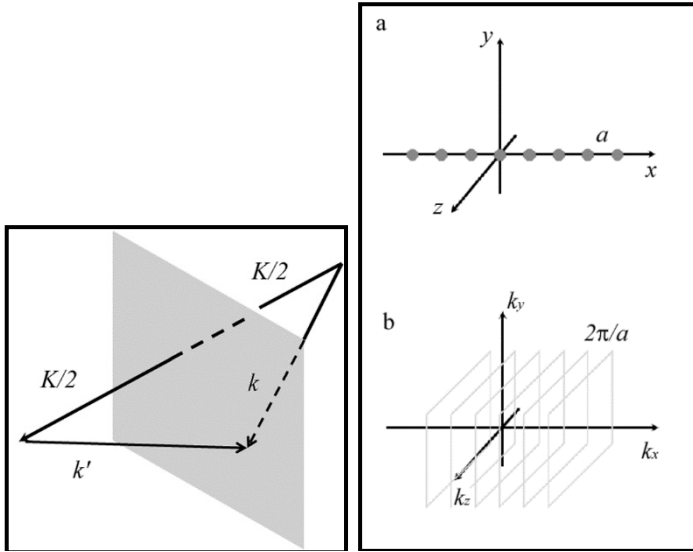


Figure 2.12: A Bragg plane is perpendicular to the vector \vec{K} and bisector of the segment $|\vec{K}|$.

Figure 2.13: A line of points in the direct space (a) is described in the reciprocal space as a family of planes (b).

From Laue's condition for a family of planes with Miller's indices $\{h, k, l\}$ we have

$$|\vec{K}_{hkl}| = \frac{2\pi n}{d_{hkl}}$$

where d_{hkl} is the distance between planes.

So the condition of constructive interference for the family of planes $\{h, k, l\}$ of the direct lattice is verified at the point (h, k, l) of the reciprocal lattice, whose projection is observed in the diffraction image.

Let us consider equally spaced points along the x axis in the direct space, as shown in Fig. 2.13 a), the density of the points of the lattice is written as

$$\rho(\vec{r}) = \delta(\vec{r} - m_1 \vec{x})$$

The Fourier transform (FT) of $\rho(\vec{r})$ is

$$\varphi(\vec{k}) = \delta\left(\vec{k} - \frac{2\pi}{a}\check{k}_x\right)$$

It represents a family of planes equally spaced in the reciprocal space, perpendicular to the k_x axis (Fig. 2.13b). These are the Bragg planes.

By considering a three-dimensional lattice in the direct space

$$\rho(\vec{r}) = \delta(\vec{r} - \vec{t}_m)$$

the FT is

$$\varphi(\vec{k}) = \delta(\vec{k} - \vec{K}_m)$$

The reciprocal lattice therefore represents the Fourier transform of the direct lattice.

The intensities of the diffraction spots are proportional to the structure factors

$$F_{\vec{K}} = \sum_j f_j e^{i\vec{K}_{hkl} \cdot \vec{r}_j}$$

where the sum runs over the elements of the basis, and f_j 's and r_j 's are their form factors and positions respectively.

A face-centred cubic lattice (fcc) can be considered as a simple cubic lattice plus a basis of four atoms that are supposed to be the same element (Fig. 2.14a). In this case

$$F_{\vec{K}} = f(1 + e^{-i\pi(h+k)} + e^{-i\pi(k+l)} + e^{-i\pi(h+l)})$$

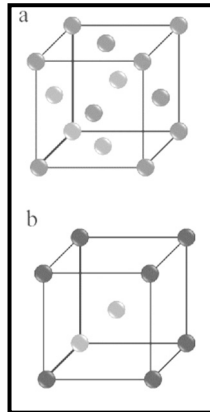


Figure 2.14: Two Bravais lattices described as a simple cubic lattice plus a basis of (a) four atoms and (b) two atoms.

Only the diffraction spots corresponding to the h, k, l indices, which may be either all even or all odd, will be seen.

A body-centred cubic lattice (bcc) can be considered as a simple cubic lattice plus a basis of two atoms that are supposed to be the same element (Fig. 2.14b). In this case

$$F_{\vec{k}} = f(1 + e^{-i\pi(h+k+l)})$$

Only the diffraction spots corresponding to families of planes with $h+k+l=\text{even}$ will be seen.

Diffraction is a powerful experimental technique that reveals order in different structures. Simple crystalline solids are the simplest examples, but surfaces (Chapter 3), macromolecules, liquid crystals (Chapter 6), etc. may also be mentioned. We will see examples in which the structure factor in a diffraction experiment can be related to the order parameter, whose change indicates the existence of a phase transition.